

Mice Lacking the USP2 Deubiquitinating Enzyme Have Severe Male Subfertility Associated with Defects in Fertilization and Sperm Motility¹

Nathalie Bedard,^{3,8} Yaoming Yang,^{3,8} Mary Gregory,^{8,9} Daniel G. Cyr,^{8,9} João Suzuki,^{4,8} Xiaomin Yu,^{4,8} Ri-Cheng Chian,^{4,8} Louis Hermo,^{5,8} Cristian O'Flaherty,^{6,8} Charles E. Smith,^{5,7,8} Hugh J. Clarke,^{4,8} and Simon S. Wing^{2,3,8}

Polypeptide Laboratory, Department of Medicine,³ Departments of Obstetrics and Gynecology,⁴ Anatomy and Cell Biology,⁵ and Urology,⁶ Facility for Electron Microscopy Research and Faculty of Dentistry,⁷ and Centre for Study of Reproduction,⁸ McGill University and McGill University Health Centre, Montreal, Quebec, Canada
INRS-Institut Armand-Frappier,⁹ Université du Québec, Laval, Quebec, Canada

ABSTRACT

The ubiquitin-proteasome system plays an important role in spermatogenesis. However, the functions of deubiquitinating enzymes in this process remain poorly characterized. We previously showed that the deubiquitinating enzyme USP2 is induced in late elongating spermatids. To identify its function, we generated mice lacking USP2. *Usp2* $-/-$ mice appeared normal, and the weights of major organs, including the testis, did not differ from wild type (*Usp2* $+/+$). However, although the numbers of testicular spermatids and epididymal spermatozoa were normal in *Usp2* $-/-$ males, these animals had a severe defect in fertility, yielding only 12% as many offspring as *Usp2* $+/+$ littermates. Spermatogenesis in *Usp2* $-/-$ mice was morphologically normal except for the presence of abnormal aggregations of elongating spermatids and formation of multinucleated cells in some tubules. The epididymal epithelium was morphologically normal in *Usp2* $-/-$ mice, but some abnormal cells other than sperm were present in the lumen. *Usp2* $-/-$ epididymal spermatozoa manifested normal motility when incubated in culture media, but rapidly became immotile when incubated in PBS in contrast to *Usp2* $+/+$ spermatozoa, which largely maintained motility under this condition. *Usp2* $-/-$ and $+/+$ spermatozoa underwent acrosome reactions *in vitro* with similar frequency. *In vitro* fertilization assays demonstrated a severe defect in the ability of *Usp2* $-/-$ spermatozoa to fertilize eggs. This could be bypassed by intracytoplasmic sperm injection or removal of the zona pellucida, which resulted in fertilization rates similar to that of *Usp2* $+/+$ mice. We demonstrate for the first time, using mouse transgenic approaches, a role for the ubiquitin system in fertilization.

fertilization, gamete biology, sperm motility and transport, ubiquitin, zona pellucida

¹Supported by the Canadian Institutes of Health Research (grants MT12121 and MOP82734 to S.S.W.; IHO94381 to H.J.C.). S.S.W. was the recipient of a Chercheur National salary award from the Fonds de la Recherche en Santé du Québec.

²Correspondence: Simon S. Wing, Polypeptide Laboratory, Strathcona Anatomy and Dentistry Bldg, Room W315, 3640 University St., Montreal, Quebec, Canada H3A 2B2. FAX: 514 398 3923; e-mail: simon.wing@mcgill.ca

Received: 14 September 2010.

First decision: 3 October 2010.

Accepted: 11 April 2011.

© 2011 by the Society for the Study of Reproduction, Inc.

This is an Open Access article, freely available through *Biology of Reproduction's* Authors' Choice option.

eISSN: 1529-7268 <http://www.biolreprod.org>

ISSN: 0006-3363

INTRODUCTION

Spermatogenesis is a complex developmental program that includes many fundamental cellular processes, such as renewal of stem cells, proliferation of spermatogonia committed to spermatogenesis, meiosis, and remodeling of the haploid round spermatids to elongated spermatids [1–3]. Spermatids released from the testis undergo further maturation during transport through the epididymis [4]. Upon ejaculation, sperm acquire the capacity to fertilize eggs. All of these steps leading to the formation of mature sperm are precisely regulated, and this regulation depends significantly on the appropriate timing of expression of specific proteins that play critical roles in mediating these events [5–7]. The steady-state level of expression of specific proteins is influenced in a major way by the transcriptional control of genes encoding these proteins, as well as by the regulation of the translation of encoded mRNAs. However, it is also critically dependent on the rates of protein degradation.

The ubiquitin-proteasome system is the major proteolytic system in the cell, responsible for the regulated degradation of many specific proteins [8]. This system plays important roles in the cell cycle, meiosis, and the terminal differentiation of various tissues. Ubiquitin is a small peptide that is covalently attached to proteins through a series of enzymatic reactions catalyzed by ubiquitin-activating enzyme, ubiquitin-conjugating enzymes, and ubiquitin protein ligases. Proteins can be monoubiquitinated (a single ubiquitin is attached at one or more lysines on the substrate) or polyubiquitinated, where a chain of multiple ubiquitin moieties is attached to the substrate. When polyubiquitin chains are attached to a protein substrate, particularly chains in which the C-terminal end of the distal ubiquitin is linked to lysine 48 in the proximal ubiquitin, the chain can mark the protein substrate for recognition and degradation by the 26S proteasome [9]. Alternatively, monoubiquitination and some non-lysine 48-linked forms of polyubiquitin chains can alter the function of the substrate protein or serve as docking sites for other proteins and thereby exert functions not mediated by proteasomal degradation [10].

Although the ubiquitin system is involved in many cellular processes, its functions during spermatogenesis remain poorly understood. In past studies, we have shown that ubiquitin conjugation is activated during spermatogenesis and that activation of conjugation is dependent on the UBC4/UBC5 family of ubiquitin-conjugating enzymes whose expression is markedly upregulated in spermatids [11]. Inactivation of the testis- and spermatid-specific UBC4-testis gene results in mice with a mild delay in postnatal growth of the testis. The HR6B/E2_{14k} isoform of UBC2 [12, 13] is expressed ubiquitously but at high levels in the testis [14]. Inactivation of this ubiquitin-

conjugating enzyme gene causes male sterility, with a heterogeneous population of abnormal spermatids as the phenotype [15].

Ubiquitin protein ligases have also been demonstrated to be involved in spermatogenesis. Mice lacking the UBR2 ligase show arrest of spermatogenesis between leptotene/zygotene and pachytene spermatocytes [16]. Inactivation of the SIAH1A ligase also results in arrest during spermatocyte development but at the metaphase to telophase transition of meiosis I [17]. The cullin ring ligase CUL3-KLHL10 is expressed in spermatids [18], and studies of the ortholog in *Drosophila* indicate that it is required for caspase activation during spermatogenesis [19]. Loss of the ligase Herc4 decreases sperm motility and fertility, and this defect is associated with defective removal of the cytoplasmic droplet from the maturing spermatid [20]. More recently, the E3 RNF8 has been shown to be essential for ubiquitination of histones and the replacement of histones by protamines during spermiogenesis [21–22].

The ubiquitin pathway also comprises enzymes that deubiquitinate target proteins. These deubiquitinating enzymes (DUBs) can play important roles in regulating ubiquitination but are poorly studied in comparison to enzymes involved in ubiquitination. DUBs have been reported to be involved in spermatogenesis. The UCH DUBs L1 and L3 both show regulated expression during spermatogenesis [23]. However, they have distinct effects, as inactivation of L1 in the mouse results in resistance to apoptosis due to heat stress of cryptorchidism, whereas inactivation of L3 shows increased sensitivity to apoptosis [24]. The CYLD DUB supports normal germ cell apoptosis, and its loss results in impaired spermatogenesis [25]. Some men with azoospermia have been found to have deletions on the Y chromosome involving the *Usp9* gene. However, men of several families with deletions of the *Usp9* gene have conceived offspring, suggesting that another gene in that region is responsible for the arrest in spermatogenesis [26, 27]. Finally, polymorphisms in *Usp26*, an X chromosome gene, have been associated with infertility [28], but whether these are indeed causative remains uncertain [29].

We previously identified two isoforms of the deubiquitinating enzyme USP2 (previously named UBp-testis) that are expressed at high levels in the testis. The two isoforms of a single gene arise from distinct promoters and the use of distinct first exons, resulting in two proteins of 43 kDa and 69 kDa that share an identical 37-kDa core catalytic domain but differ in their N-terminal extensions. Expression of USP2 isoforms in the testis is highly regulated, with both isoforms induced in late elongating spermatids [30]. The N-terminal extensions target the enzyme to distinct cellular compartments and confer substrate selectivity [30, 31]. Although much cellular characterization has been carried out on this enzyme, the physiological functions remain unknown. To explore the function of USP2 in vivo, we therefore targeted the gene for inactivation in the mouse and have identified a fertility defect in male mice.

MATERIALS AND METHODS

All procedures were carried out in accordance with the regulations of the Canadian Council for Animal Care and were approved by the Animal Care Committees of McGill University, the McGill University Health Centre, and the Institut Armand Frappier.

Creation of Transgenic Mice Lacking USP2

The *Usp2* gene-targeting construct was generated using the recombination cloning method [32]. Adjacent intronic sequences of ~120 bp between exons 7 and 8 were inserted in the pLoxP-Tc-LoxP plasmid immediately upstream and downstream of LoxP sites flanking a tetracycline selection cassette. The modified plasmid was transformed into the recombination-proficient bacterial

strain SCRNI10. These cells were then infected with the λ K0-2 *129/SvEvBrd* bacteriophage mouse genomic library containing mouse genomic inserts of 10–14 kb. Each genomic insert is located adjacent to a thymidylate kinase gene (TK1), and the two are flanked by R recombinase target sequences sites to generate a loopout plasmid upon induction of the recombinase in SCRNI10 cells with isopropyl- β -D-thio-galactoside. A clone containing exons 2 to 11 of the *Usp2* gene (Fig. 1A) was isolated by selection with tetracycline. The isolated clone was transformed into the bacterial strain BNN132 expressing Cre recombinase to excise the tetracycline cassette, leaving one LoxP site between exons 6 and 7. To insert the second LoxP site and a mammalian selection cassette, the pKOEZ plasmid was digested with *AseI* and *NheI*, releasing a 2.9-kb fragment containing a neomycin/kanamycin selection cassette flanked by Flp recombinase target sequences (Frt) and a LoxP sequence just distal to the Frt sequence adjacent to the neomycin gene. Adjacent intronic sequences between exons 3 and 4 of the *Usp2* gene were amplified by PCR, ligated to each side of the 2.9-kb cassette, and inserted into a pGEM cloning vector for amplification. The modified fragment bearing the cassette with adjacent intronic sequences was excised, purified, and electroporated into recombination-proficient DH10 β bacterial strain previously transformed with the *Usp2* phage clone isolated from BNN132 cells. After selecting for kanamycin-resistant clones, the final plasmid was purified, linearized, and electroporated into embryonic stem (ES) cells. Growth of the cells in the presence of G418 and FIAU selected for the presence of the neomycin resistance gene and the absence of the thymidylate kinase gene (provided by the λ K0-2 library clone)—events that would occur as a result of appropriate homologous recombination across the two flanks. Cells from two different clones were then injected into mouse blastocysts and reimplanted in pseudopregnant female C57BL/6 mice (The Jackson Laboratory). Chimeric male mice were backcrossed with C57BL/6 females to identify mice in which germ line transmission of the mutant allele had taken place. These heterozygotes were then crossed with transgenic mice expressing Cre recombinase under the control of the cytomegalovirus (CMV) promoter to excise exons 4–6 encoding part of the catalytic core domain, including the critical active site cysteine residue. Mice in which the excision was successful were further backcrossed with C57BL/6 mice, and the resulting heterozygotes were mated to obtain homozygous knockout males and wild-type littermates. Some of the studies were carried out using heterozygotes that were derived from mice that had also been crossed with mice expressing the Flp recombinase to remove the selection cassette. Similar defects in fertility were observed independently of the presence or absence of the selection cassette.

Polymerase Chain Reactions

Genomic DNA was isolated from the tails of mice and genotyped by PCR (Fig. 1B). To detect the *Usp2*^{+/+} allele, oligonucleotides (5'-GGTTGAAGC CAGGCATG-3' and 5'-AGGGCTCTCATCTTGAG-3') on each side of the downstream LoxP site (located between exons 6 and 7) were used in PCR (1 min denaturation at 94°C, 1 min annealing at 48°C, 30 sec extension at 72°C, 35 cycles). The *Usp2*^{+/+} allele generates a 229-bp product. The *Usp2*^{-/-} allele does not generate any product because the binding site of the forward primer is lost upon Cre recombinase-mediated excision. To confirm the excision of exons 4–6 in the *Usp2*^{-/-} allele, oligonucleotides (5'-CGCATGCTCCAGACTGCCTT-3' and 5'-AGGGCTCTCATCTTGAG-3'), located in the selection cassette and downstream of the LoxP site, respectively, were used in PCR (1 min denaturation at 94°C, 1 min annealing at 48°C, 30 sec extension at 72°C, 35 cycles). The *Usp2*^{-/-} allele generated a 250-bp product (due to excision of exons 4–6), whereas the *Usp2*^{+/+} allele did not generate any product, the two primers being separated by >2.5 kb.

To measure *Usp2* mRNA expression, RNA was isolated from *Usp2*^{+/+} or *Usp2*^{-/-} testis using the guanidium isothiocyanate method and treated with reverse transcriptase to prepare cDNA. The cDNA was then used as template in PCR with oligonucleotides 5'-GGTCTGGCTGGTCTTCGAAAC-3' and 5'-CCTTCCAGATACTTCTCC-3', derived from exons 3 and 7, respectively, which amplified 425- and 78-bp products in *Usp2*^{+/+} or *Usp2*^{-/-}, respectively. A confirmatory PCR reaction was also carried out using oligonucleotides 5'-CCAGAGATATGCACCAC-3' and 5'-GGAACCTCTG GACAGAGA-3', derived from exons 4 and 10, respectively, which amplified a product (450 bp) only in the *Usp2*^{+/+} sample. Finally, a positive control PCR was carried out with oligonucleotides 5'-GGAGGAAGTATCTGGAAAGG-3' and 5'-GTCACCTCAGGGTAACCAC-3', derived from exons 7 and 9, respectively, and this resulted in a 165-bp product in both genotypes. A control reaction in which reverse transcriptase was omitted gave a negative result in all PCR reactions.

Immunoblotting

Mouse embryonic fibroblasts were prepared from Postcoital Day 13.5 embryos as previously described [33]. Mouse embryonic fibroblasts were

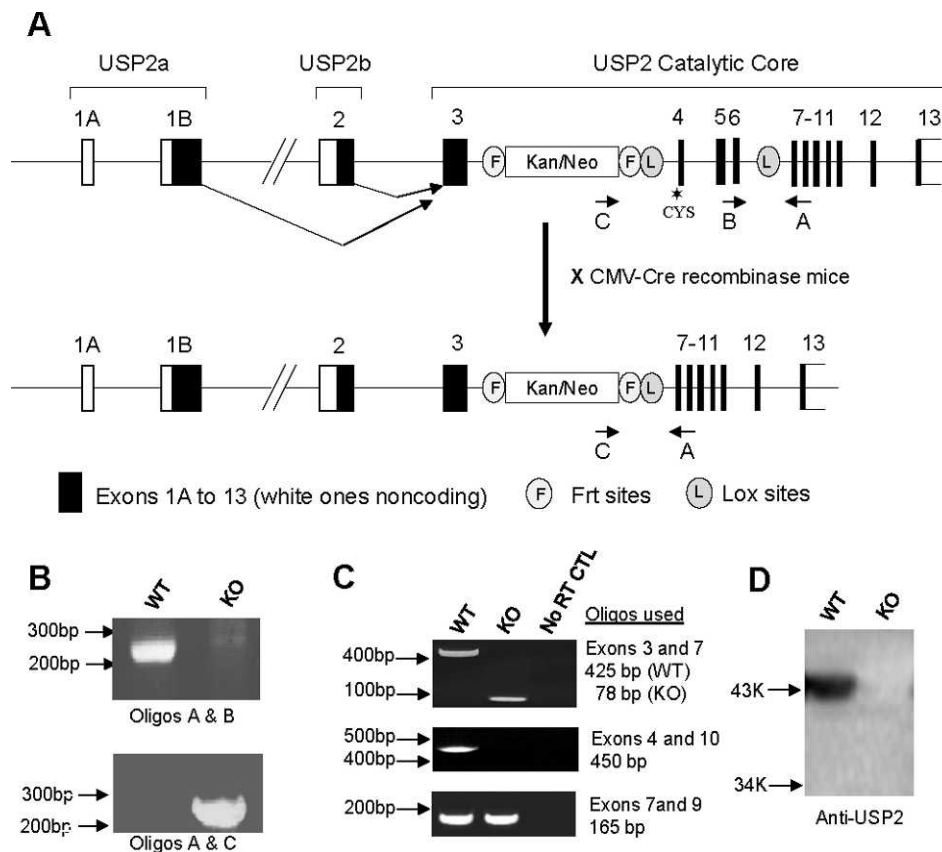


FIG. 1. Generation of *Usp2*^{-/-} mice. **A**) ES cells were targeted with a vector that, upon recombination, inserted LoxP sites upstream of exon 4 and downstream of exon 6 and a selection cassette between exons 3 and 4 of the *Usp2* gene. Mice derived from these ES cells were backcrossed with C57BL/6 mice to produce offspring bearing a copy of this modified *Usp2* allele in the germ line. These mice were crossed with mice expressing Cre recombinase under the ubiquitous CMV promoter to excise exons 4–6 containing the active site CYS. These heterozygous (HT) mice were then bred to obtain *Usp2*^{+/+}, HT, or *Usp2*^{-/-} mice. **B**) PCR on tail genomic DNA of offspring from crosses of HT mice demonstrating successful excision of exons 4–6 in *Usp2*^{-/-} mice. Positions of oligonucleotides used in PCR are indicated in **A**. **C**) RT-PCR on testis RNA from *Usp2*^{+/+} and *Usp2*^{-/-} mice using primers from the indicated exons. Indicated on the right are the sizes of the expected products. PCR products from *Usp2*^{-/-} were smaller compared to *Usp2*^{+/+} when using primers in exons 3 and 7, confirming the efficient excision of exons 4, 5, and 6 in *Usp2*^{-/-}. Products were absent in *Usp2*^{-/-} when a primer from the deleted exon 4 was used but were present when primers from exons 7 and 9 (downstream of the excision) were used. Controls were reactions in which reverse transcriptase had been omitted. **D**) Western blot of protein of lysates obtained from *Usp2*^{+/+} or *Usp2*^{-/-} embryonic fibroblasts using anti-*Usp2* antibodies.

grown in Dulbecco modified Eagle medium supplemented with 10% fetal bovine serum, penicillin-streptomycin, and glutamine (Gibco). The cells were lysed in 20 mM Tris-Cl (pH 8.0), 1% Triton X-100, 5 mM ethylenediaminetetraacetic acid, 150 mM NaCl, 5 mM NaF, 5 mM Na pyrophosphate, 1 mM Na₃VO₄, 1 mM PMSF, 5 mM N-ethylmaleimide, and protease inhibitor cocktail (Roche). Protein (100 µg) was subjected to SDS-PAGE on 5%–10% gradient gels and transferred to polyvinylidene fluoride membranes. These membranes were incubated with rabbit anti-USP2 antibody (C-terminal L523; Abgent) diluted 1:333, followed by goat anti-rabbit antibody and chemiluminescence detection using a cooled digital camera (BioRad). Immunoblotting, immunohistochemistry, and fluorescence on testis and sperm samples was attempted using this antibody as well as four different rabbit antisera against the catalytic core region without success.

In Vivo Fertility Assays

Male *Usp2*^{-/-} mice or their heterozygous (+/-) or +/+ littermates were mated with CD1 females (Charles River) starting at age 6 wk for either 5 mo or 6 wk. The female mouse was changed each week. Litter number and size were counted. Fertilization rates were also measured using superovulated females. Male *Usp2*^{-/-} or +/+ mice were each mated with two CD1 females that had been superovulated by i.p. injection of 10 IU equine chorionic gonadotropin (Sigma Chemicals), followed 48 h later by 5 IU of human chorionic gonadotropin (hCG; Sigma). The next day, females were killed, the eggs were harvested and cultured, and the number of fertilized eggs was counted.

In Vitro Fertilization

Adult CD1 female mice were superovulated as described above and killed 16 h after hCG. Oviducts were dissected into a Petri dish containing prewarmed HEPES-buffered modified human tubal fluid (mHTF; pH 7.2) washing medium, supplemented with 1.0 mg/ml bovine serum albumin (BSA; Sigma A8806). Cumulus masses were released by tearing the ampullae of the oviducts then were transferred into 50-µl fertilization droplets (bicarbonate-buffered mHTF, supplemented with 4.0 mg/ml BSA) under oil. Each droplet received one cumulus mass.

Male *Usp2*^{-/-} and +/+ mice were killed, and the caudae epididymides and vas deferens were removed. Sperm were directly squeezed from the caudae epididymides into a 40-µl droplet under mineral oil of mHTF supplemented with 9 mg/ml BSA to induce capacitation. Sperm were incubated for 60–90 min at 37°C in a humidified atmosphere of 5% CO₂ in air. These now-capacitated spermatozoa were added to the fertilization droplet at a sperm concentration of 1–25 × 10⁶ sperm per milliliter. To assess dispersion of the layer of cumulus cells, the eggs were visualized using a microscope and photographed at the indicated time points. For regular in vitro fertilization, gametes were co-incubated for 6 h, following which each zygote was transferred into a 50-µl droplet of Embryo Maintenance Medium (EMM; Cooper Surgical/SAGE) for development. The following day, embryos that developed to the two-cell stage were identified and recorded. To assess the ability of sperm to fertilize zona pellucida-free eggs, immature oocytes were collected by follicular puncture and incubated overnight as previously described [34]. The following day, any adhering cumulus cells were removed by aspirating the oocytes using a narrow-bore glass micropipette.

A

Breeding for 5 months

♂	# of Litters	Litter Size	# Pups
WT	20	11.7 ± 0.9	234
KO	6	4.7 ± 1.8	28

Breeding for 5 weeks

♂	# of Litters	Litter Size	# Pups
WT	9	12.3 ± 0.7	111
HT	5	12.2 ± 1.0	61
KO	1	2	2

B

	# Matings	#Plugs	%Plugging	# Litters	# Pups
WT (n=5)	24	15	63	10	116
KO (n=6)	27	15	56	2	8

C

	Total # Eggs	# Fertilized (%)	# Unfertilized (%)	# Others (%) (parthenogenetically activated or fragmented)
WT (n=4)	157	75 (48%)	56 (36%)	26 (17%)
KO (n=4)	189	20 (8.7%)	131 (69%)	38 (20%)

D

♀ USP2	# of Litters	Mean Litter Size
WT	6	8.5 +/- 0.7
KO	7	9.4 +/- 0.2

Oocytes that had reached metaphase II, as indicated by the presence of a polar body, were then incubated in acid Tyrode (Sigma) for about 10 sec until the zona pellucida disappeared. The zona pellucida-free eggs were washed in preequilibrated mHTF medium and incubated with spermatozoa as described above for the *in vitro* fertilization procedure.

Intracytoplasmic Sperm Injection

Caudae epididymides from *Usp2* *+/+* and *-/-* mice were isolated and placed in HEPES-buffered mHTF, and the large tubules were cut to allow the spermatozoa to diffuse into the medium. Equal parts of the sperm suspension were mixed thoroughly with HEPES-buffered mHTF containing 12% (w/v) polyvinylpyrrolidone (360 kDa; Sigma). Micromanipulation was performed using an inverted microscope (Olympus IX 70; Olympus) equipped with a heating plate (Tokai Hit, Japan), and temperature was maintained at 25°–30°C for all manipulations. The sperm head was separated from the tail by applying several Piezo (Piezo PMM prime tech; Piezo) pulses. Sperm heads (5–10) were isolated and loaded into the injection pipette and then injected singly into individual oocytes according to the method described by Kimura and Yanagimachi [35]. The sperm suspension was replaced every 30 min during the intracytoplasmic sperm injection (ICSI) procedure. Injected oocytes were placed in 20- μ l drops of HEPES-buffered mHTF covered with mineral oil and kept at room temperature for 10 min to permit the plasma membrane to heal. Following an additional 20-min incubation in bicarbonate-buffered HTF at 37°C in a humidified atmosphere of 5% CO₂ in air, surviving oocytes were transferred to EMM and cultured as described above.

Acrosome Reaction

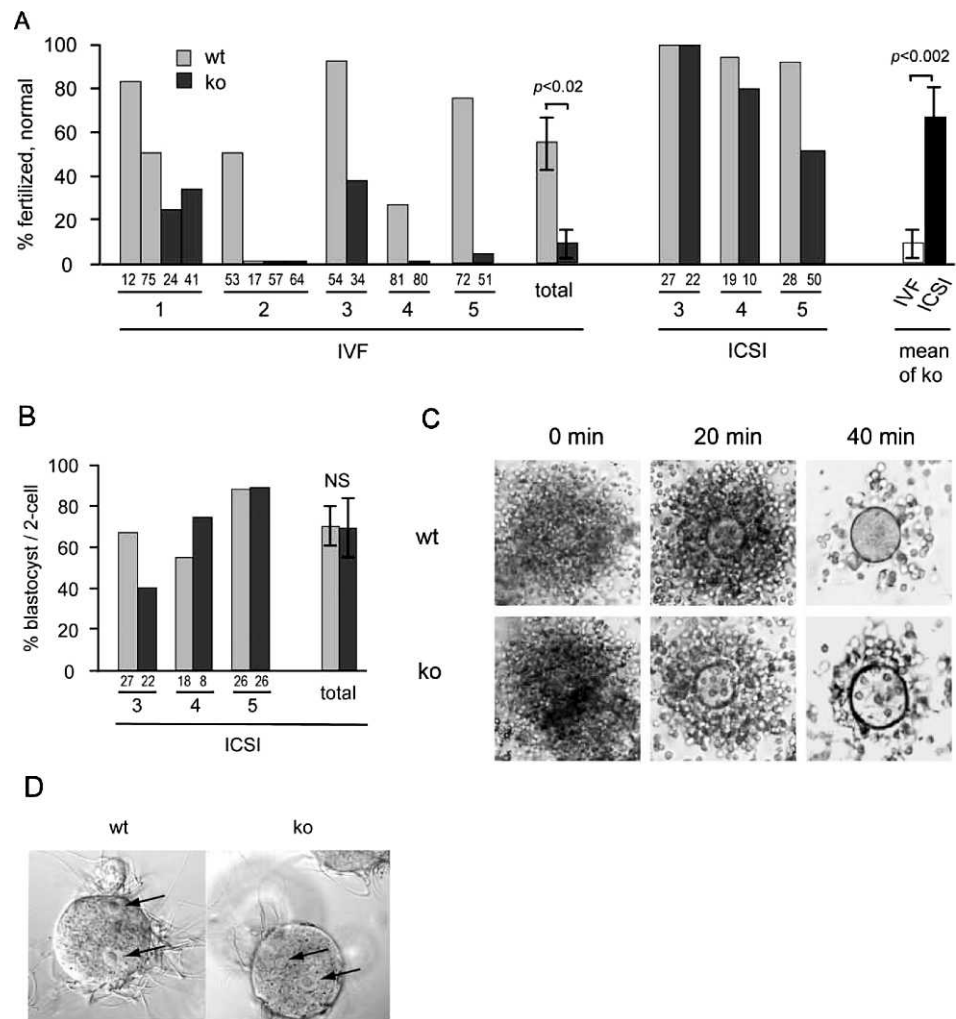
Caudae epididymides from both *Usp2* *+/+* or *-/-* mice were isolated and placed in 1 ml noncapacitating media (10 mM HEPES [pH 7.4], 95 mM NaCl, 4.8 mM KCl, 1.2 mM MgSO₄, 1.2 mM KH₂PO₄, 20 mM sodium lactate, 5 mM glucose, and 0.25 mM sodium pyruvate). The cauda region was pierced using a surgical blade to allow sperm to disperse into the medium, and the sperm were incubated at 37°C for 10 min. The sperm were counted, spun at 350 × *g* for 10 min, and resuspended in noncapacitating or capacitating media (noncapacitating media supplemented with 1.3 mM CaCl₂, 25 mM NaHCO₃, 0.3% BSA, and NaCl adjusted to 120 mM) to a concentration of 5 × 10⁶ cells per milliliter. The sperm suspension was incubated for 3 h at 37°C. To induce the acrosome reaction, the sperm were treated with 15 μ M progesterone (Sigma) or vehicle (dimethyl sulfoxide) for the final 15 min of the incubation. The sperm were finally fixed in 4% paraformaldehyde for 15–30 min, spun at 350 × *g* for 10 min, and smeared onto a microscope slide. The air-dried samples were stained with 0.22% Coomassie blue G-250 for 5 min, rinsed in water, dried, and mounted. Intact acrosomes were identified by their intense staining. Two hundred sperm from each sample were analyzed for the presence or absence of an intact acrosome by an observer who did not know the genotypes of the samples.

Motility Assays

Caudae epididymides from *Usp2* *+/+* or *-/-* mice were isolated and placed in prewarmed Hanks medium M199 (Invitrogen Canada Inc.) supplemented with 3 mg/ml BSA at 37°C [36]. The cauda region was pierced using a surgical blade to allow sperm to disperse into the medium and incubated for 5 min on a

FIG. 2. **A**) Severe reduction in fertility in *Usp2* *-/-* males. Male *Usp2* *-/-* mice or their HT or *+/+* littermates were mated with CD1 females starting at age 6 wk for either 5 mo (one *+/+* and one *-/-* male studied) or 6 wk (two *+/+*, one HT, and three *-/-* males studied). The female mouse was changed each week. Indicated are the number of litters sired and the average litter sizes. Shown are means ± SEM. Similar defect also seen with C57BL/6 females (data not shown). **B**) Reduction in fertility is not due to inability to inseminate. Male *Usp2* *-/-* or *+/+* mice were mated with CD1 females who were examined for the presence of a vaginal plug each day. Although percentage of plugging is similar with *Usp2* *+/+* or *-/-*, litter number and size are severely reduced in *Usp2* *-/-*. **C**) Fertilization rate tested using superovulated females. Male *Usp2* *-/-* or *+/+* mice were each mated with two CD1 females who had been hormonally superovulated. The next day, females were killed, the eggs were harvested and cultured, and the number of fertilized eggs was counted. *Usp2* *-/-* males yielded only 12% of the number of fertilized eggs obtained with *Usp2* *+/+* males. **D**) *Usp2* *-/-* females have normal fertility. *Usp2* *+/+* or *-/-* females (both mixed sv129/C57BL6) were mated with *Usp2* *+/+* CD1 males. Litters were readily obtained with each genotype. Indicated are mean litter sizes.

FIG. 3. Spermatozoa from *Usp2* $-/-$ mice are defective in in vitro fertilization (IVF) but have normal capacities to disperse the cumulus layer and to fertilize eggs following ICSI or incubation with zona pellucida-free eggs. **A, B**) Embryonic development following IVF or ICSI using sperm from *Usp2* $+/+$ (wt) or $-/-$ (ko) males. **A**) Fertilization. Eggs were inseminated, and the number of healthy fertilized eggs was recorded at the one-cell stage (experiment 2) or the two-cell stage (experiments 1, 3–5). Numbers at the base of each column show the number of eggs examined. IVF and ICSI of *Usp2* $-/-$ embryos compared in the far-right pair of bars. Shown are the mean rates of fertilization obtained with each procedure. **B**) Development to blastocyst following ICSI. The fraction of two-cell embryos that reached the blastocyst stage is shown. Numbers at the base of each column show the number of two-cell embryos. **C**) Cumulus dispersal. *Usp2* $+/+$ or $-/-$ spermatozoa were incubated with egg masses and photographed at the indicated times to assess dispersal of the layer of cumulus cells. Shown are representative images; original magnification $\times 10$ (left and middle panels) and $\times 20$ (right panels). **D**) Fusion with zona pellucida-free eggs. *Usp2* $+/+$ or $-/-$ spermatozoa were incubated with eggs from which the cumulus cells and zona pellucida had been removed. Six hours later, eggs were fixed, stained with propidium iodide, and examined using bright-field and fluorescence microscopy. Eggs containing two or more pronuclei were classified as fertilized. Shown are representative bright-field images with arrows indicating the pronuclei. *Usp2* $+/+$, 27 of 30 eggs fertilized; *Usp2* $-/-$, 30 of 32 eggs fertilized. Original magnification $\times 40$.



37°C plate. The sperm suspension was transferred to a microfuge tube and centrifuged at $350 \times g$ for 10 min. The sperm pellet was gently resuspended in either Hanks medium M199 or PBS, both supplemented with 3 mg/ml BSA and incubated at 37°C. Aliquots of sperm were taken at various time points, diluted twofold with the same media, and placed in a prewarmed 80- μ m glass chamber for Computer-Assisted Sperm Analysis (IVOS automated semen analyzer; Hamilton Thorne Biosciences). Statistical analyses, including Shapiro-Wilk tests for normality, Grubb tests for detecting outliers, and Mann-Whitney tests (nonparametric test) were done using Statistica for Windows Version 9 (Statsoft, Inc.). In all cases, *P*-values less than 0.05 were considered significant. Graphs of results from motility analyses were plotted as means \pm 95% confidence intervals.

Light Microscopy

The indicated tissues were isolated and fixed in 10% neutral buffered formalin at 4°C for 24 h. After fixation, the samples were dehydrated in ethanol prior to paraffin embedding. Sections (4 μ m) were cut from the embedded samples and stained with hematoxylin and eosin.

RESULTS

Creation of Transgenic Mice Lacking *Usp2*

Since our previous studies demonstrated marked induction of USP2 expression in late elongating spermatids, we further explored its function during spermatogenesis by generating mice lacking USP2. To allow for future conditional inactivation studies, mice were generated in which a loxP recombination site was inserted in the intron upstream of exon 4 and also

in an intron downstream of exon 6 (Fig. 1A). Exon 4 contains the essential active site cysteine residue, so deletion of exons 4–6 will result in inactivation of *Usp2*. In order to obtain an initial global test of USP2 function, we induced whole body inactivation of *Usp2* by crossing our mice bearing a targeted allele with mice expressing Cre recombinase under the control of the ubiquitous CMV promoter. These heterozygous mice were then backcrossed with C57BL/6 mice for at least three generations before being used in breeding to generate homozygous *Usp2* $-/-$ mice and $+/+$ littermates (Fig. 1B). Mice homozygous for loss of *Usp2* were born in the expected Mendelian ratio (data not shown), indicating that USP2 is not essential for development during gestation. Expression analysis confirmed that *Usp2* mRNA was absent in the testis (Fig. 1C) of *Usp2* $-/-$ mice. Levels of USP2 in all tissues tested from *Usp2* $+/+$ mice were too low to be reliably detected by Western blotting or by immunohistochemical and immunofluorescent staining of the testis and spermatozoa, respectively. However, Western blot analysis of protein from mouse embryonic fibroblasts did identify specifically the 45-kDa USP2b isoform in *Usp2* $+/+$ but not from *Usp2* $-/-$ samples, confirming the loss of USP2 protein (Fig. 1D).

Usp2 Knockout Mice Have a Defect in Fertility

Mice lacking USP2 were normal in appearance. Weights of major organs of *Usp2* $-/-$ mice were similar to those in *Usp2*

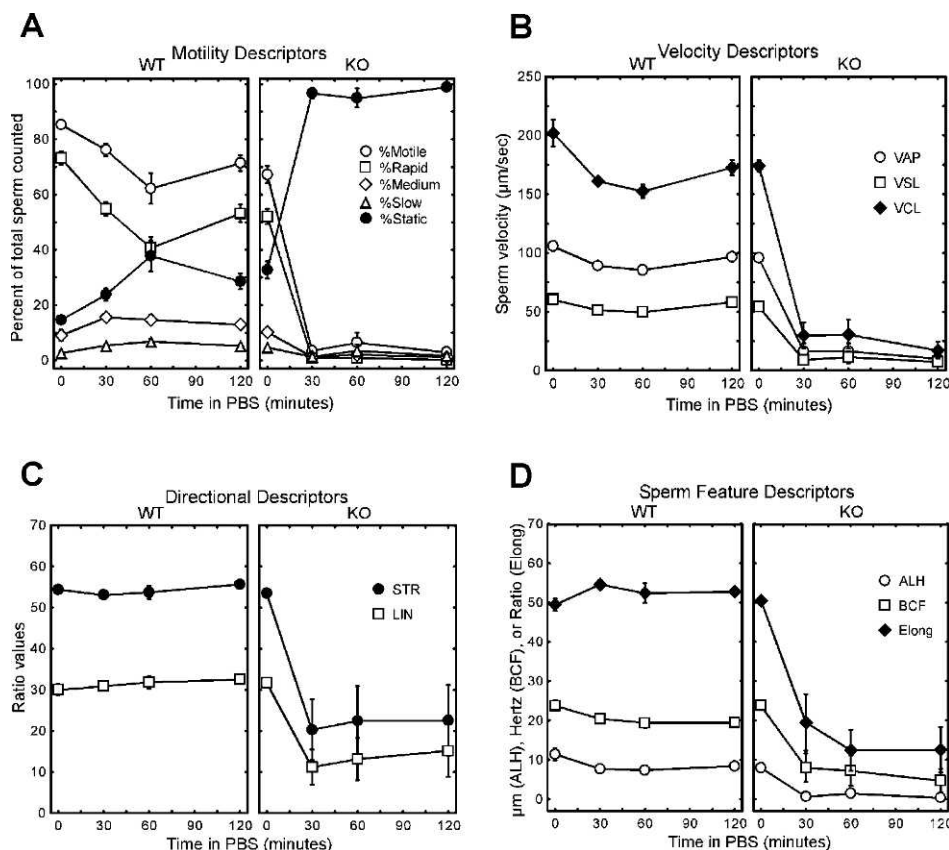


FIG. 4. *Usp2*^{-/-} spermatozoa show defects in motility. Spermatozoa were isolated from the cauda epididymis of either *Usp2*^{+/+} or *-/-* mice. Following incubation in M199 media with 3 mg/ml BSA for 5 min, the spermatozoa were collected by low-speed centrifugation and resuspended gently in PBS. Aliquots were then removed at the indicated time points and analyzed by computer-assisted sperm analysis. **A**) Distributions of motile sperm. **B**) Velocity parameters: VAP, average path velocity; VSL, straight line velocity; VCL, curvilinear velocity. **C**) Parameters of directional motion: STR, straightness (VSL/VAP \times 100); LIN, linearity (VSL/VCL \times 100). **D**) Sperm motion features: ALH, amplitude of lateral head displacement; BCF, beat cross frequency; Elong, ratio of minor to major axes of the sperm head. Shown are means and 95% confidence intervals. Where the error bars are not visible, they were smaller than the graph point marker.

+/+ mice (Supplemental Fig. S1 available online at www.biolreprod.org). However, mating of the *USP2*^{-/-} males quickly revealed that these mice had a major defect in fertility. Compared to *Usp2*^{+/+} littermates, *Usp2*^{-/-} males rarely sired litters. Moreover, the average litter size was less than 50% that of normal males. The infrequent and smaller litters resulted in an 88%–98% reduction in overall progeny generated by the *Usp2*^{-/-} males (Fig. 2A). This marked decrease in fertility was not due to a decrease in copulatory behavior of the *Usp2*^{-/-} males, as the frequency of vaginal plugging by these animals was similar to that of *Usp2*^{+/+} controls (Fig. 2B). To test whether decreased fertility was due to a failure of fertilization, we determined the number of eggs fertilized in superovulated females 1 day after mating with *Usp2*^{+/+} or *-/-* males (Fig. 2C). Mating with normal male mice resulted in almost 50% of the eggs being fertilized. In contrast, less than 10% of the eggs were fertilized following mating with *Usp2*^{-/-} males. This 85% decrease in fertility corresponds closely to the decrease in fertility seen with natural mating with nonsuperovulated females (Fig. 2A). Fertility of *Usp2*^{-/-} females was normal (Fig. 2D), implying that the defect in fertility is not due to general abnormalities in the hypothalamic-pituitary axis.

Spermatozoa from Usp2 Knockout Mice Are Defective in Fertilization

To elucidate the basis for the failed fertilization, we studied the function of spermatozoa isolated from the cauda epididymis. Importantly, the number of epididymal spermatozoa was similar in *Usp2*^{+/+} and *-/-* mice, indicating that the subfertility was not due to decreased sperm number (Supple-

mental Fig. S1 available online at www.biolreprod.org). We tested the ability of the spermatozoa to fertilize eggs in vitro. Approximately 60% of eggs were fertilized by *Usp2*^{+/+} spermatozoa, whereas only approximately 10% of eggs were fertilized by *-/-* spermatozoa (Fig. 3A). The failure of sperm of *Usp2*^{-/-} males to fertilize eggs could be due to a failure to reach the egg, fuse with the plasma membrane, or activate the egg following penetration into the cytoplasm. To discriminate between these possibilities, we used ICSI to directly introduce the sperm into the egg cytoplasm. We found that 80% of the oocytes injected with *-/-* spermatozoon divided to generate a two-cell embryo (Fig. 3B). Moreover, a similar fraction of two-cell embryos (about 70%) produced using *Usp2*^{+/+} and *-/-* sperm were able to reach the blastocyst stage (Fig. 3B). These results indicate that the *Usp2*^{-/-} sperm were capable of activating eggs to begin embryonic development. Therefore, their inability to fertilize eggs in vivo or in vitro probably reflects a failure to reach the egg or to fuse with its plasma membrane.

The first step toward reaching the egg is for the sperm to induce dispersion of the surrounding cumulus cells. *Usp2*^{+/+} or *-/-* sperm were incubated with cumulus egg masses, and the dispersion of the cumulus was monitored by light microscopy over time (Fig. 3C). Both *Usp2*^{+/+} and *-/-* sperm induced rapid dispersal of the cumulus cells within 40 min, indicating that *Usp2*^{-/-} sperm are normal in this function. The final step is fusion with the egg. To test whether there was a defect at this step, zona pellucida-free eggs were incubated with *Usp2*^{+/+} or *-/-* sperm (Fig. 3D). Sperm from both genotypes fertilized these eggs with equal efficiency (*Usp2*^{+/+}, 90%; *Usp2*^{-/-}, 94%), indicating that loss of

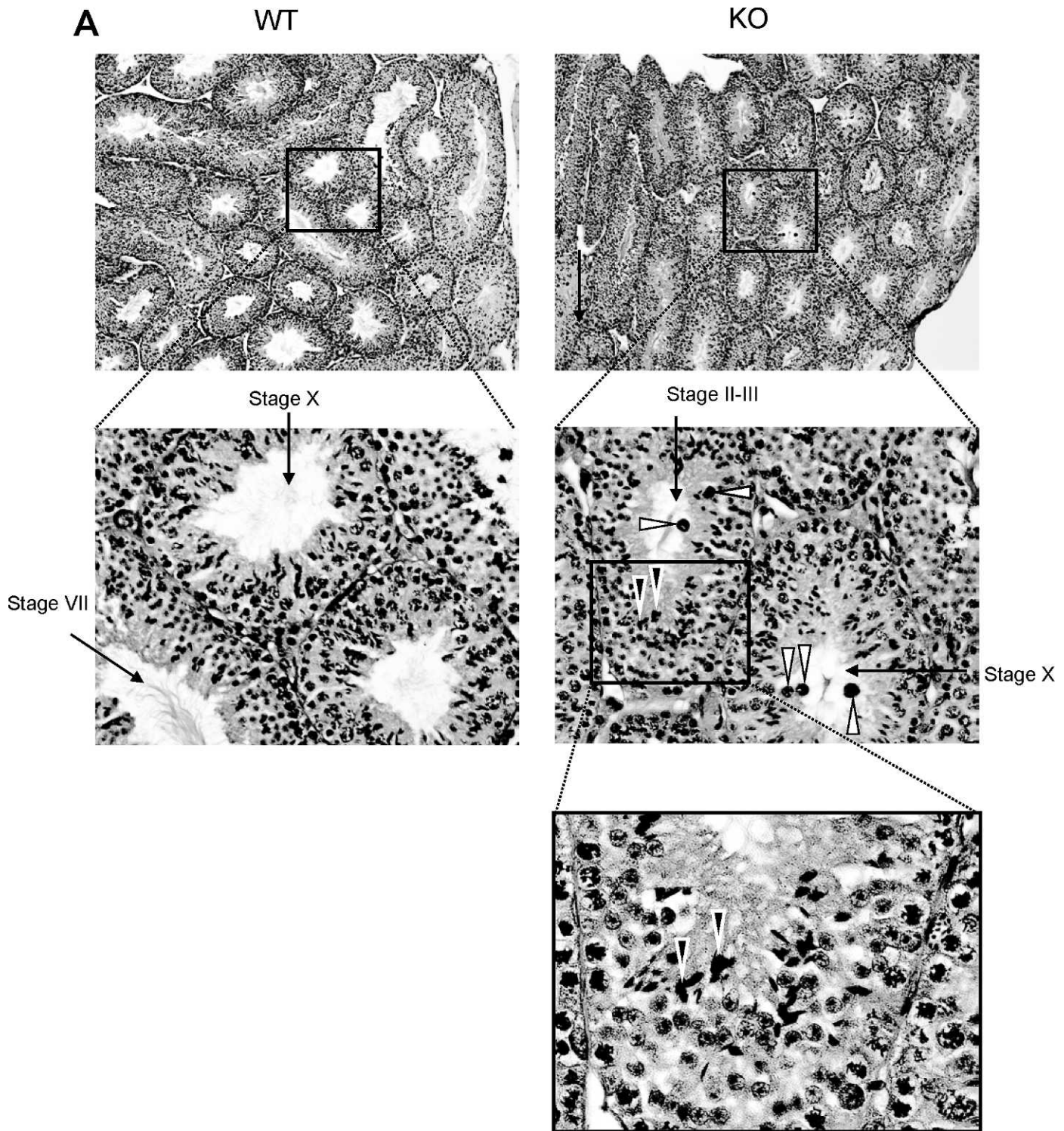


FIG. 5. *Usp2*^{-/-} mice show subtle defects in late stage maturation of spermatids in the testis. **A**) Shown are representative sections of the testis stained with hematoxylin and eosin and viewed with low (top) or high (bottom) magnification. Note in bottom the abnormal clustering of elongating spermatids (black arrowheads) and the round structures that are most likely multinucleated cells/bodies (white arrowheads). **B**) Overall normal morphologic appearance of the epididymis. Top panel: low-power magnification of the cauda of the epididymis from *Usp2*^{+/+} or *-/-* mice. Middle and lower panels: high-power magnifications of the cauda from *Usp2*^{+/+} or *-/-* mice. Arrowheads indicate, in the *Usp2*^{-/-}, probable multinucleated cells derived from aberrant maturation of elongating spermatids. **C**) Dark field images of epididymal spermatozoa from *Usp2*^{+/+} or *-/-* mice. No evident differences seen. Original magnifications are as follows: For **A**, $\times 10$ (top), $\times 40$ (middle), and $\times 100$ (bottom); for **B**, $\times 10$ (top), $\times 40$ (middle), and $\times 100$ (bottom); and for **C**, $\times 40$.

USP2 does not prevent binding to and fusion with the egg. Therefore, the marked impairment in fertilization capacity observed *in vitro* must be due to a defect in binding to or penetration of the zona pellucida.

Acrosome Reaction

Since binding of sperm to the zona pellucida activates the acrosome reaction and the exocytosis of acrosomal contents is

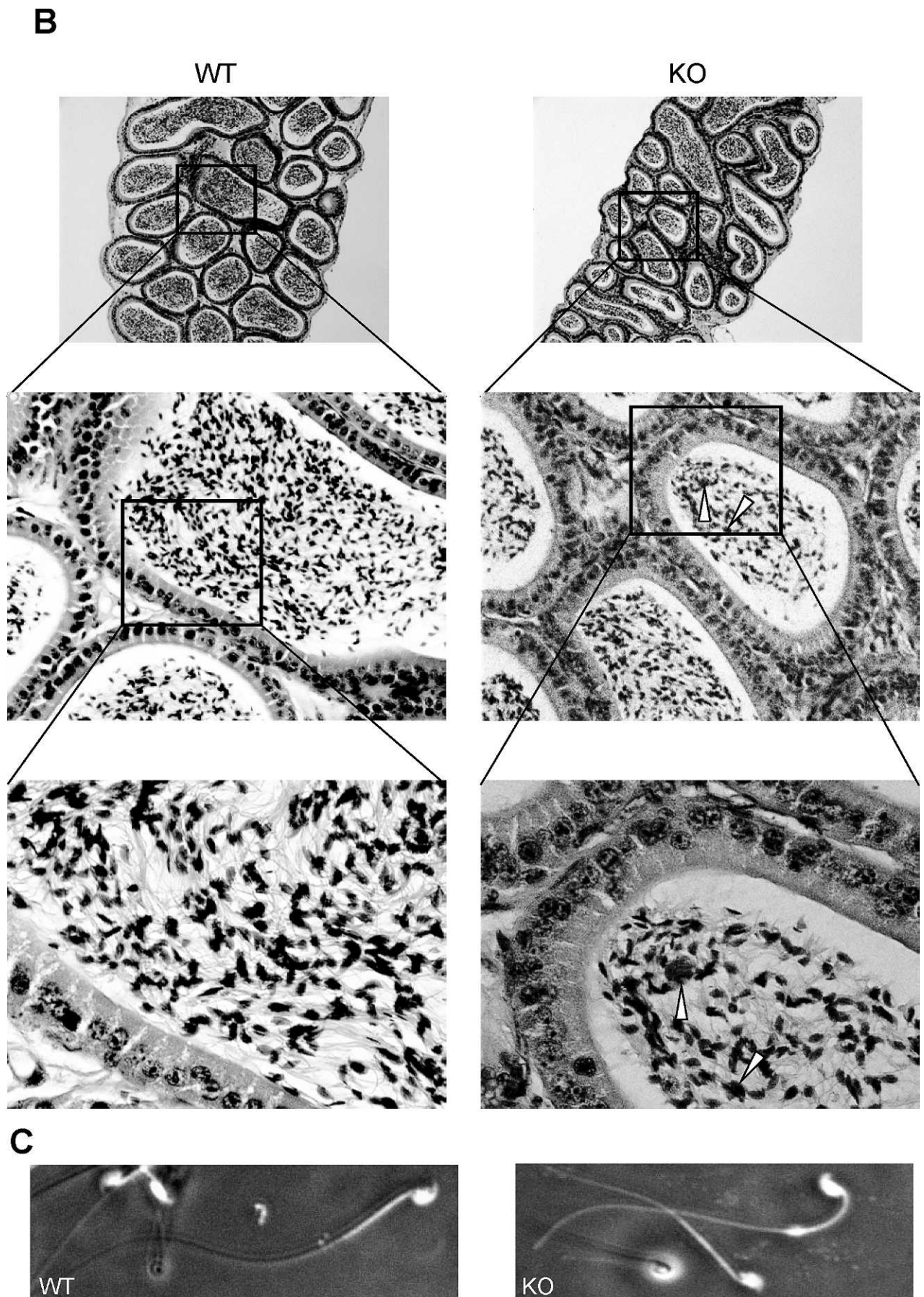


FIG. 5. Continued.

necessary for zona penetration and binding to the egg, we tested whether *Usp2*^{-/-} sperm undergo an acrosome reaction upon capacitation and stimulation with progesterone. After incubation for 3 h, 53% ± 3.5% of the sperm had undergone the acrosome reaction, similar to the 59% ± 4.5% of *Usp2*^{+/+} sperm.

Motility of Spermatozoa from *Usp2*^{-/-} Mice

Since a defect in sperm motility was also possible, we assessed this directly by using computer-assisted sperm analysis to study spermatozoa isolated from the caudae epididymides of *Usp2*^{+/+} and *Usp2*^{-/-} mice and capacitated in vitro. When spermatozoa from *Usp2*^{+/+} or *Usp2*^{-/-} mice were incubated in Hanks M199 medium with 3 mg/ml BSA for 5 min to activate motility (time = 0 in Fig. 4), most of the spermatozoa were observed to be highly motile. Slightly more of the *Usp2*^{+/+} spermatozoa than *Usp2*^{-/-} spermatozoa were initially motile (85% vs. 67%), and correspondingly more of the *Usp2*^{-/-} than *Usp2*^{+/+} spermatozoa were immotile (33% vs. 15%). Average path velocity (VAP), straight line velocity (VSL), curvilinear velocity (VCL), and amplitude of lateral head displacement (ALH) were slightly lower compared to *Usp2*^{+/+}, but these differences were very small (<15%) and of unlikely biological importance. Indeed, these small differences in descriptors of motility and velocity were not consistently seen from experiment to experiment. In most experiments, incubation of *Usp2*^{+/+} or *Usp2*^{-/-} spermatozoa in capacitating media for up to 4 h yielded motility values that were similar in the two genotypes (Supplemental Fig. S2 available online at www.biolreprod.org). Linearity of movement as well as ALH were similar between *Usp2*^{+/+} and *Usp2*^{-/-} mice, suggesting that hyperactivation occurred normally in *Usp2*^{-/-} mice. Indeed, hyperactivated spermatozoa could be readily detected from both genotypes after 2 h of incubation in Hanks M199 medium (Supplemental Fig. S3 available online at www.biolreprod.org).

Since sperm is deposited in the reproductive tract that has a fluid environment different from that of the media, we explored whether defects in function might be evident under less optimal environmental conditions. We isolated spermatozoa from *Usp2*^{+/+} or *Usp2*^{-/-} epididymides in capacitating media and then transferred the spermatozoa into PBS, which is deficient in nutrients as well as in ions such as Ca²⁺, Mg²⁺, and HCO₃⁻. Spermatozoa from *Usp2*^{+/+} mice remained largely active, with only a slight (~10%) decrease in the number of motile sperm over the 2-h observation period (Fig. 4). Rapidly motile sperm decreased by 30% over the same period, with resulting increases in the percentages of medium, slow, and static sperm. There were small but significant decreases over the first 30 min in VAP, VSL, VCL, ALH, and beat cross frequency (BCF). In contrast to *Usp2*^{+/+} sperm, which maintained motility, sperm from *Usp2*^{-/-} mice showed a precipitous decrease in all motility parameters within 30 min of incubation in PBS. The percentage of motile sperm decreased dramatically, with over 95% of the sperm becoming completely immotile. This was not due to cell death, as the number of nonviable cells as assessed by trypan blue staining were small (<1%) and similar in both *Usp2*^{+/+} and *Usp2*^{-/-} spermatozoa after 60 min of incubation.

Morphology of the Testis, Epididymis, and Spermatozoa

To begin exploring the basis for this defect in motility, we analyzed the morphology of spermatids throughout their developmental stages in intact testes (Fig. 5). Using light

microscopy, the testis of the *Usp2*^{-/-} mice showed a normal organization of the seminiferous epithelium (Fig. 5A). However, near the lumen, there was evidence of abnormal aggregation of elongating spermatids and formation of multinucleated cells in some seminiferous tubules. Spermatozoa in the lumen appeared normal except for the increased presence of multinucleated bodies similar to those identified in the sections of the testis (Fig. 5A). Analysis of the epididymides from *Usp2*^{-/-} mice by light microscopy (Fig. 5B) also revealed a normal epithelium, save for the occasional presence of multinucleated cells similar to those seen in the testis. Finally, the morphology of spermatozoa isolated from the cauda epididymidis appeared normal (Fig. 5C).

DISCUSSION

In this report, we have described for the first time using gene inactivation in vivo functions of the USP2 deubiquitinating enzyme. USPs are the largest family of deubiquitinating enzymes [37], encoded by ~65 genes, and to date, inactivation in the mouse has been reported for only three of them: USP18 [38], USP8 [39], and CYLD [25, 40]. Male mice lacking *Usp2* showed a severe defect in fertility. However, spermatogenesis was not altered significantly, as revealed by light microscopy analysis. Though subtle abnormalities in spermiogenesis, such as the presence of some aggregated late elongating spermatids and the presence of multinucleated bodies in the lumen, were observed in some tubules (Fig. 5), these abnormalities were infrequent and did not result in a decrease in sperm number. Thus, the subfertility noted in the *Usp2*^{-/-} mice did not result from defects in sperm production.

Instead, subfertility appeared due to a major defect in the ability of the sperm to fertilize eggs, as demonstrated by both in vivo and in vitro fertility assays (Figs. 2 and 3). This defect was overcome by intracytoplasmic injection of the sperm, confirming that the abnormality was in the fertilization process. The initial step in this process, dispersion of the cumulus, was normal using *Usp2*^{-/-} sperm. The final steps, binding to and fusion with the egg plasma membrane, were similarly normal. Therefore, the defect lies at the level of the zona pellucida, either in binding to or in penetration of this egg vestment. Previous studies have implicated a role of the ubiquitin proteasome system in fertilization [41]. When incubated in the presence of a proteasome inhibitor, pig sperm are unable to penetrate the zona pellucida of co-incubated eggs. However, if the zona is removed from the eggs, fertilization proceeds even in the presence of the proteasome inhibitor [42], indicating a role for the proteasome in penetration of the zona, as occurs in the ascidian *Halocynthia roretzi* [43]. Zona proteins in porcine eggs appear to be ubiquitinated [42] and, therefore, consistent with a model in which they are substrates for proteasome-mediated degradation. Addition of the nonspecific deubiquitinating enzyme inhibitor, Ub-aldehyde, to porcine in vitro fertilization assays promotes polyspermy, which may be related to enhanced ubiquitination and degradation of the zona pellucida [44]. Our data are an important complement to the above studies using inhibitors by providing the first genetic evidence for a role of the UPS in fertilization. The exact mechanisms by which USP2 supports binding or penetration of the zona pellucida remain unclear.

Penetration of the zona pellucida is believed to be dependent on a combination of sperm motility and release of hydrolytic enzymes occurring due to the acrosomal reaction. Both *Usp2*^{+/+} and *Usp2*^{-/-} spermatozoa underwent similar rates of acrosome reaction upon incubation in capacitating medium. It remains possible, though, that zona-induced acrosome reaction may be

defective in *Usp2* $-/-$ sperm, and this remains to be tested. *Usp2* $-/-$ sperm had similar motility to $+/+$ sperm when incubated in complete media similar to that used in the in vitro fertilization assays. However, upon incubation in PBS, *Usp2* $-/-$ sperm rapidly lost motility, indicating that a defect in motility does exist and can be made manifest under more demanding conditions. The requirement for spermatozoa to penetrate the viscous zona pellucida may represent such a challenging condition and correlates well with our observation that *Usp2* $-/-$ spermatozoa are unable to penetrate this layer of the egg vestments in vitro.

The mechanism underlying the motility defect remains to be determined. Sperm from *Usp2* $+/+$ littermates remained largely motile for at least 2 h in the absence of nutrients, indicating that they have the endogenous ability to generate adequate chemical energy and to transform that chemical energy into mechanical action. The rapid loss of motility of *Usp2* $-/-$ sperm upon transfer to nutrient-deficient medium strongly suggests a defect in the ability to generate chemical energy. Previous work indicates that mouse sperm generates most of its ATP from glycolysis [45, 46]. The source of endogenous energy for motility in the absence of an exogenous energy source is unclear. Long-chain acyl CoA esters have been suggested as a possible source [47]. Glycogen has been reported to be present in canine spermatozoa [48] but was not detected in rodent spermatozoa [49]. It is possible that *Usp2* $-/-$ spermatozoa metabolize glucose less efficiently and have lower steady state ATP levels than *Usp2* $+/+$ spermatozoa. Upon transfer to nutrient-deficient medium, the lower basal ATP levels in *Usp2* $-/-$ spermatozoa may fall rapidly below a threshold required for motility and penetration of the egg vestments. Interestingly, previous studies have implicated a role for ubiquitination in regulating sperm motility. Mice lacking the ubiquitin ligase *Herc4* [20] reveal largely normal-appearing sperm morphologically, but with a defect in fertility and motility. Our studies elaborate on this theme by demonstrating for the first time a role for a deubiquitinating enzyme in regulation of sperm motility.

The normal incubation medium differs from PBS not only in energy substrate, but also in ions such as calcium and bicarbonate. Both of these ions are important for switching on key signaling pathways that are important for activation and hyperactivation of sperm. Inactivation of several voltage-gated calcium channels leads to defects in sperm motility [50, 51]. HCO_3^- is also required for acquisition of normal motility upon capacitation [52]. These two ions activate soluble adenylate cyclase, which generates cAMP, leading to activation of protein kinase A and subsequently activation of tyrosine kinases. Inactivation of the soluble adenylate cyclase in the mouse leads to infertility and severely impaired motility [53]. Calcium fluxes also activate calmodulin-dependent kinases, and pharmacologic inhibition of calmodulin-dependent kinases leads to impaired motility [54]. The *Usp2* $+/+$ spermatozoa may be able to maintain calcium fluxes during incubation in PBS by using intracellular stores of calcium such as the redundant nuclear envelope [55, 56]. It may be that the $-/-$ spermatozoa are unable to properly regulate calcium release from such stores. Further mechanistic insights will require supplementation studies to identify the minimal components in the M199 medium that are essential for maintaining or restoring motility in the *Usp2* $-/-$ spermatozoa.

An additional approach toward determining the mechanism would be to identify the substrates of USP2. This would require the identification of proteins that are destabilized or more highly ubiquitinated in the *Usp2* $-/-$ spermatozoa as compared to the *Usp2* $+/+$ spermatozoa. Some of these substrates could

form complexes with the enzyme, so identification of proteins that interact with USP2 would also be of interest. Recently, a high-throughput, large-scale identification of the proteins that interact with deubiquitinating enzymes was reported [57]. Surprisingly, there were relatively few proteins identified as high-probability interactors with USP2, and of those identified, none appears to be involved in sperm motility. A limiting aspect is that the large-scale screen was carried out in HEK293 cells. There are large differences in the profile of proteins expressed in these cells as compared to spermatozoa, and the functions of USPs can be highly dependent on the cellular context.

During spermatid maturation in the testis, the nucleus undergoes condensation and the chromatin becomes tightly packed into the spermatid head. This results in the arrest of gene transcription in the early elongating spermatids. Thus, subsequent development, maturation of the spermatids, and function of the resulting spermatozoa are highly dependent on posttranscriptional regulation. Combined with our previous studies indicating that USP2 is expressed in late elongating spermatids [30], these studies indicate that regulation of ubiquitination of proteins by the USP2 deubiquitinating enzyme may be one such important regulatory mechanism and is essential for fertilization.

ACKNOWLEDGMENT

We thank Marie Plourde for technical assistance.

REFERENCES

1. Clermont Y. Kinetics of spermatogenesis in mammals: seminiferous epithelium cycle and spermatogonial renewal. *Physiol Rev* 1972; 52:198–236.
2. Hermo L, Pelletier RM, Cyr DG, Smith CE. Surfing the wave, cycle, life history, and genes/proteins expressed by testicular germ cells, part 1: background to spermatogenesis, spermatogonia, and spermatocytes. *Microsc Res Tech* 2010; 73:241–278.
3. Hermo L, Pelletier RM, Cyr DG, Smith CE. Surfing the wave, cycle, life history, and genes/proteins expressed by testicular germ cells, part 2: changes in spermatid organelles associated with development of spermatozoa. *Microsc Res Tech* 2010; 73:279–319.
4. Orgebin-Crist MC. Studies on the function of the epididymis. *Biol Reprod* 1969; 1(suppl 1):155–175.
5. Hecht NB. Regulation of 'haploid expressed genes' in male germ cells. *J Reprod Fertil* 1990; 88:679–693.
6. Hermo L, Pelletier RM, Cyr DG, Smith CE. Surfing the wave, cycle, life history, and genes/proteins expressed by testicular germ cells, part 4: intercellular bridges, mitochondria, nuclear envelope, apoptosis, ubiquitination, membrane/voltage-gated channels, methylation/acetylation, and transcription factors. *Microsc Res Tech* 2010; 73:364–408.
7. Hermo L, Pelletier RM, Cyr DG, Smith CE. Surfing the wave, cycle, life history, and genes/proteins expressed by testicular germ cells, part 5: intercellular junctions and contacts between germ cells and Sertoli cells and their regulatory interactions, testicular cholesterol, and genes/proteins associated with more than one germ cell generation. *Microsc Res Tech* 2010; 73:409–494.
8. Glickman MH, Ciechanover A. The ubiquitin-proteasome proteolytic pathway: destruction for the sake of construction. *Physiol Rev* 2002; 82:373–428.
9. Chau V, Tobias JW, Bachmair A, Marriott D, Ecker DJ, Gonda DK, Varshavsky A. A multiubiquitin chain is confined to specific lysine in a targeted short-lived protein. *Science* 1989; 243:1576–1583.
10. Hochstrasser M. Ubiquitin signalling: what's in a chain? *Nat Cell Biol* 2004; 6:571–572.
11. Rajapurohitam V, Morales CR, El-Alfy M, Lefrancois S, Bédard N, Wing SS. Activation of a UBC4-dependent pathway of ubiquitin conjugation during postnatal development of the rat testis. *Dev Biol* 1999; 212: 217–228.
12. Wing SS, Dumas F, Banville D. A rabbit reticulocyte ubiquitin carrier protein that supports ubiquitin-dependent proteolysis (E214k) is homol-

- ogous to the yeast DNA repair gene RAD6. *J Biol Chem* 1992; 267:6495–6501.
13. Koken MH, Reynolds P, Jaspers-Dekker I, Prakash L, Prakash S, Bootsma D, Hoeijmakers JH. Structural and functional conservation of two human homologs of the yeast DNA repair gene RAD6. *Proc Natl Acad Sci USA* 1991; 88:8865–8869.
 14. Wing SS, Banville D. 14-kDa ubiquitin-conjugating enzyme: structure of the rat gene and regulation upon fasting and by insulin. *Amer J Physiol* 1994; 267:E39–E48.
 15. Roest HP, van Klaveren J, de Wit J, van Gurp CG, Koken MHM, Vermey M, van Roijen JH, Hoogerbrugge JW, Vreeburg JTM, Baarends WM, Bootsma D, Grootegoed JA, et al. Inactivation of the HR6B ubiquitin-conjugating DNA repair enzyme in mice causes male sterility associated with chromatin modification. *Cell* 1996; 86:799–810.
 16. Kwon YT, Xia Z, An JY, Tasaki T, Davydov IV, Seo JW, Sheng J, Xie Y, Varshavsky A. Female lethality and apoptosis of spermatocytes in mice lacking the UBR2 ubiquitin ligase of the N-end rule pathway. *Mol Cell Biol* 2003; 23:8255–8271.
 17. Dickins RA, Frew IJ, House CM, O'Bryan MK, Holloway AJ, Haviv I, Traficante N, de Kretser DM, Bowtell DD. The ubiquitin ligase component Siah1a is required for completion of meiosis I in male mice. *Mol Cell Biol* 2002; 22:2294–2303.
 18. Wang S, Zheng H, Esaki Y, Kelly F, Yan W. Cullin3 is a KLHL10-interacting protein preferentially expressed during late spermiogenesis. *Biol Reprod* 2006; 74:102–108.
 19. Arama E, Bader M, Rieckhof GE, Steller H. A ubiquitin ligase complex regulates caspase activation during sperm differentiation in *Drosophila*. *PLoS Biol* 2007; 5:e251.
 20. Rodriguez CI, Stewart CL. Disruption of the ubiquitin ligase HERC4 causes defects in spermatozoon maturation and impaired fertility. *Dev Biol* 2007; 312:501–508.
 21. Lu LY, Wu J, Ye L, Gavrilina GB, Saunders TL, Yu X. RNF8-dependent histone modifications regulate nucleosome removal during spermatogenesis. *Dev Cell* 2010; 18:371–384.
 22. Li L, Halaby MJ, Hakem A, Cardoso R, El Ghamrasni S, Harding S, Chan N, Bristow R, Sanchez O, Durocher D, Hakem R. Rnf8 deficiency impairs class switch recombination, spermatogenesis, and genomic integrity and predisposes for cancer. *J Exp Med* 2010; 207:983–997.
 23. Kwon J, Wang YL, Setsuie R, Sekiguchi S, Sakurai M, Sato Y, Lee WW, Ishii Y, Kyuwa S, Noda M, Wada K, Yoshikawa Y. Developmental regulation of ubiquitin C-terminal hydrolase isozyme expression during spermatogenesis in mice. *Biol Reprod* 2004; 71:515–521.
 24. Kwon J, Wang YL, Setsuie R, Sekiguchi S, Sato Y, Sakurai M, Noda M, Aoki S, Yoshikawa Y, Wada K. Two closely related ubiquitin C-terminal hydrolase isozymes function as reciprocal modulators of germ cell apoptosis in cryptorchid testis. *Am J Pathol* 2004; 165:1367–1374.
 25. Wright A, Reiley WW, Chang M, Jin W, Lee AJ, Zhang M, Sun SC. Regulation of early wave of germ cell apoptosis and spermatogenesis by deubiquitinating enzyme CYLD. *Dev Cell* 2007; 13:705–716.
 26. Krausz C, Degl'Innocenti S, Nuti F, Morelli A, Felici F, Sansone M, Variale G, Forti G. Natural transmission of USP9Y gene mutations: a new perspective on the role of AZFa genes in male fertility. *Hum Mol Genet* 2006; 15:2673–2681.
 27. Luddi A, Margollicci M, Gambera L, Serafini F, Cioni M, De Leo V, Balestri P, Piomboni P. Spermatogenesis in a man with complete deletion of USP9Y. *N Engl J Med* 2009; 360:881–885.
 28. Stouffs K, Lissens W, Tournaye H, Van Steirteghem A, Liebaers I. Possible role of USP26 in patients with severely impaired spermatogenesis. *Eur J Hum Genet* 2005; 13:336–340.
 29. Stouffs K, Lissens W, Tournaye H, Van Steirteghem A, Liebaers I. Alterations of the USP26 gene in Caucasian men. *Int J Androl* 2006; 29:614–617.
 30. Lin H, Keriel A, Morales CR, Bedard N, Zhao Q, Hingamp P, Lefrançois S, Combaret L, Wing SS. Divergent N-terminal sequences target an inducible testis deubiquitinating enzyme to distinct subcellular structures. *Mol Cell Biol* 2000; 20:6568–6578.
 31. Lin H, Yin L, Reid J, Wilkinson KD, Wing SS. Effects of divergent amino terminal sequences of a deubiquitinating enzyme on substrate specificity. *J Biol Chem* 2001; 276:20357–20363.
 32. Zhang P, Li MZ, Elledge SJ. Towards genetic genome projects: genomic library screening and gene-targeting vector construction in a single step. *Nat Genet* 2002; 30:31–39.
 33. Nagy A, Gertsenstein M, Vintersten K, Behringer R. Preparing mouse embryo fibroblasts. *Cold Spring Harb Protoc*; 2006; doi:10.1101/pdb.prot4398.
 34. Yang Q, Allard P, Huang M, Zhang W, Clarke HJ. Proteasomal activity is required to initiate and to sustain translational activation of messenger RNA encoding the stem-loop-binding protein during meiotic maturation in mice. *Biol Reprod* 2010; 82:123–131.
 35. Kimura Y, Yanagimachi R. Development of normal mice from oocytes injected with secondary spermatocyte nuclei. *Biol Reprod* 1995; 53:855–862.
 36. Slott VL, Suarez JD, Perreault SD. Rat sperm motility analysis: methodologic considerations. *Reprod Toxicol* 1991; 5:449–458.
 37. Nijman SM, Luna-Vargas MP, Velds A, Brummelkamp TR, Dirac AM, Sixma TK, Bernards R. A genomic and functional inventory of deubiquitinating enzymes. *Cell* 2005; 123:773–786.
 38. Malakhov MP, Malakhova OA, Kim KI, Ritchie KJ, Zhang DE. UBP43 (USP18) specifically removes ISG15 from conjugated proteins. *J Biol Chem* 2002; 277:9976–9981.
 39. Niendorf S, Oksche A, Kisser A, Lohler J, Prinz M, Schorle H, Feller S, Lewitzky M, Horak I, Knobloch KP. Essential role of ubiquitin-specific protease 8 for receptor tyrosine kinase stability and endocytic trafficking in vivo. *Mol Cell Biol* 2007; 27:5029–5039.
 40. Reiley WW, Jin W, Lee AJ, Wright A, Wu X, Tewalt EF, Leonard TO, Norbury CC, Fitzpatrick L, Zhang M, Sun SC. Deubiquitinating enzyme CYLD negatively regulates the ubiquitin-dependent kinase Tak1 and prevents abnormal T cell responses. *J Exp Med* 2007; 204:1475–1485.
 41. Zimmerman S, Sutovsky P. The sperm proteasome during sperm capacitation and fertilization. *J Reprod Immunol* 2009; 83:19–25.
 42. Sutovsky P, Manandhar G, McCauley TC, Caamano JN, Sutovsky M, Thompson WE, Day BN. Proteasomal interference prevents zona pellucida penetration and fertilization in mammals. *Biol Reprod* 2004; 71:1625–1637.
 43. Sakai N, Sawada MT, Sawada H. Non-traditional roles of ubiquitin-proteasome system in fertilization and gametogenesis. *Int J Biochem Cell Biol* 2004; 36:776–784.
 44. Yi YJ, Manandhar G, Sutovsky M, Li R, Jonakova V, Oko R, Park CS, Prather RS, Sutovsky P. Ubiquitin C-terminal hydrolase-activity is involved in sperm acrosomal function and anti-polyspermy defense during porcine fertilization. *Biol Reprod* 2007; 77:780–793.
 45. Miki K, Qu W, Goulding EH, Willis WD, Bunch DO, Strader LF, Perreault SD, Eddy EM, O'Brien DA. Glyceraldehyde 3-phosphate dehydrogenase-S, a sperm-specific glycolytic enzyme, is required for sperm motility and male fertility. *Proc Natl Acad Sci U S A* 2004; 101:16501–16506.
 46. Mukai C, Okuno M. Glycolysis plays a major role for adenosine triphosphate supplementation in mouse sperm flagellar movement. *Biol Reprod* 2004; 71:540–547.
 47. Carey JE, Olds-Clarke P, Storey BT. Oxidative metabolism of spermatozoa from inbred and random bred mice. *J Exp Zool* 1981; 216:285–292.
 48. Ballester J, Fernandez-Novell JM, Rutllant J, Garcia-Rocha M, Jesus Palomo M, Mogas T, Pena A, Rigau T, Guinovart JJ, Rodriguez-Gil JE. Evidence for a functional glycogen metabolism in mature mammalian spermatozoa. *Mol Reprod Dev* 2000; 56:207–219.
 49. Anderson WA, Personne P. The localization of glycogen in the spermatozoa of various invertebrate and vertebrate species. *J Cell Biol* 1970; 44:29–51.
 50. Ren D, Navarro B, Perez G, Jackson AC, Hsu S, Shi Q, Tilly JL, Clapham DE. A sperm ion channel required for sperm motility and male fertility. *Nature* 2001; 413:603–609.
 51. Qi H, Moran MM, Navarro B, Chong JA, Krapivinsky G, Krapivinsky L, Kirichok Y, Ramsey IS, Quill TA, Clapham DE. All four CatSper ion channel proteins are required for male fertility and sperm cell hyperactivated motility. *Proc Natl Acad Sci U S A* 2007; 104:1219–1223.
 52. Ho HC, Granish KA, Suarez SS. Hyperactivated motility of bull sperm is triggered at the axoneme by Ca²⁺ and not cAMP. *Dev Biol* 2002; 250:208–217.
 53. Esposito G, Jaiswal BS, Xie F, Krajnc-Franken MA, Robben TJ, Strik AM, Kuil C, Philipsen RL, van Duin M, Conti M, Gossen JA. Mice deficient for soluble adenylyl cyclase are infertile because of a severe sperm-motility defect. *Proc Natl Acad Sci U S A* 2004; 101:2993–2998.
 54. Ignatz GG, Suarez SS. Calcium/calmodulin and calmodulin kinase II stimulate hyperactivation in demembrated bovine sperm. *Biol Reprod* 2005; 73:519–526.
 55. Ho HC, Suarez SS. An inositol 1,4,5-trisphosphate receptor-gated intracellular Ca²⁺ store is involved in regulating sperm hyperactivated motility. *Biol Reprod* 2001; 65:1606–1615.
 56. Ho HC, Suarez SS. Characterization of the intracellular calcium store at the base of the sperm flagellum that regulates hyperactivated motility. *Biol Reprod* 2003; 68:1590–1596.
 57. Sowa ME, Bennett EJ, Gygi SP, Harper JW. Defining the human deubiquitinating enzyme interaction landscape. *Cell* 2009; 138:389–403.